文章编号: 1001 - 9014(2017)02 - 0149 - 05 DOI:10.11972/j.issn.1001 - 9014.2017.02.005

Focal shift of silicon microlens array in mid-infrared regime

ZUO Hai-Jie[1], YANG Wen[1], ZHANG Jiang-Yong[1], YING Lei-Ying[1],
ZHANG Bao-Ping[1*], HOU Zhi-Jin[2], CHEN Hong-Xu[2], SI Jun-Jie[2]

(1. Laboratory of Micro/Nano Optoelectronics, Department of Electronic Engineering, Xiamen University, Xiamen 361005, China;
2. Luoyang Optoelectro Technology Development Center, Luoyang 471009, China)

Abstract: In this study rigorous numerical model was utilized to characterize the focal shift of the diffractive mid-infrared (MIR) silicon microlens arrays (MLAs) with the critical size smaller than the working wavelength. We found a more pronounced focal shift in mid-infrared wavelength which is out of the range predicted by existing models. Focal properties of the MLAs were also measured experimentally. The results agrees well with the simulation results. Our results provide a reference point in understanding the focal shift in MIR regime, which is important in terms of deciding the focal length of micro-nano lens systems, especially when dealing with the integration of diffractive devices in infrared optical system.

Key words: sub-wavelength structure, FDTD, infrared detector, focal shift, microlens array
PACS: 42.79.-e, 42.25.Fx

中红外硅微透镜阵列的离焦效应

左海杰[1], 杨 文[1], 张江勇[1], 应磊莹[1], 张保平[1*], 侯治锦[2], 陈洪许[2], 司俊杰[2]

(1. 厦门大学 电子工程系 微纳光电子研究室,福建 厦门 361005;
2. 洛阳光电技术研究中心, 河南 洛阳 471009)

摘要:采用严格数值算法对中红外硅微透镜阵列进行了模拟,该微透镜阵列特征尺寸小于波长工作波长.研究发现该微透镜阵列存在一个显著的离焦效应,其离焦量达到0.4左右,超出了现有的传统理论模型预测范围.对微透镜阵列进行了制作和焦距测试,发现测试结果跟数值模拟基本吻合.微纳衍射光学集成系统中透镜离焦量是系统集成非常重要的一个参数,该研究结果为硅微透镜阵列和中红外探测器光学集成提供有效参考.

关 键 词:亚波长结构;FDTD;红外探测器;离焦;微透镜阵列

中图分类号:TN214 **文献标识码**:A

Introduction

The popularization of micro-nano fabrication techniques, such as lithography and induced coupled plasma (ICP) etching, has provided the scientific community with a variety of new micro diffractive optical components that can be fabricated[1-3] and integrated into many new and standard applications: from imaging to light concentration, such as solid state image sensors[4-6], detectors[7], solar cells and LEDs[8]. Being compatible with standard semiconductor fabrication process[9], the physical dimension of these devices can be within the range of several wavelengths. Further miniaturization of these devices, however, can lead to deterioration of focal properties, thus hindering the application in micro optical systems. One hindrance is the widely known phenomena, the focal shift[10], namely the difference between actual focal length and the designed one.

Over the decades, extensive efforts have been devoted to explore the properties of the focal shift and its effects on the integration in optical systems[4, 11-15]. Si MLAs[16-17] are usually employed in image sensor systems because of their high optical transmittance and stable

Received date: 2016-06-09, **revised date**: 2016-12-13 **收稿日期**:2016-06-09, **修回日期**:2016-12-13

Foundation items: Supported by Special Project on the Integration of Industry, Education and Research of Aviation Industry Corporation of China (CXY2011XD24)

Biography: ZUO Hai-Jie (1988-), male, Henan Zhengzhou, Ph. D. candidate. Research fields focus on micro/nano optoelectronics devices. E-mail: hjzuoo@126.com

* **Corresponding author**: E-mail: bzhang@xmu.edu.au

thermal and mechanical properties. Most studies, however, were focused in the visual or near-infrared wavelengths. There were few papers in the literature that studied this phenomenon in the mid-infrared (MIR), where the applied wavelength was about several times longer than visible counterparts. In this case these devices are more likely to be effected by near field diffraction and scattering, and lead to deterioration of focal properties which existing models usually fail to predict. As a result, rigorous methods must be utilized for the focal length modeling.

Classical diffraction theories were usually adopted to perform the calculation of the focal shift in previous studies, however, it is known that traditional analysis models should be precluded when the dimension of optical devices reaches to the order of or smaller than the illumination wavelength. In order to generate a more accurate understanding of the focal shift in the wavelength scale, rigorous numerical method 3D Finite-Difference Time-Domain (FDTD) was employed to study the focal shift phenomena of silicon MLAs in MIR. Based on our simulation, silicon MLAs were then fabricated and corresponding measurements were carried out to characterize focal shift properties. To our knowledge this is the first time the focal shift has been studied numerically and experimentally in the MIR.

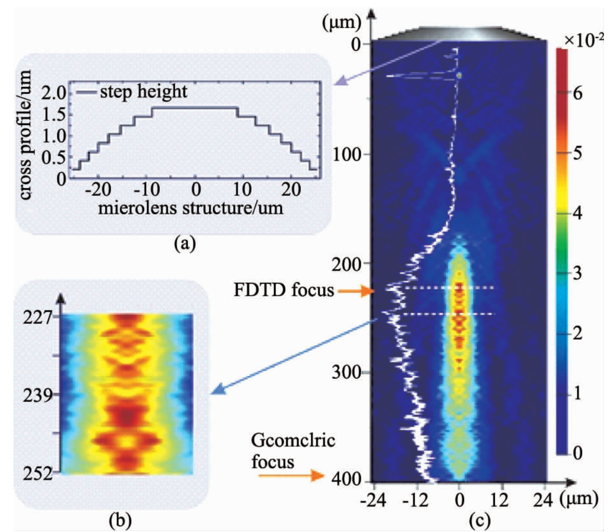

Fig. 1 Schematic simulation setup and power distribution of silicon MLA. (a) Geometry of multistep microlens, (b) magnified details of focal properties, (c) power distribution along wave illumination direction (z-axis)

图 1 微透镜阵列模拟结构和光能分布:(a)多台阶结构微透镜,(b)焦点区域放大图,(c)光强随入射光 z 方向分布

1 Numerical calculation

Traditional analysis models employing scalar calculation were usually used to analysis the properties of microlens such as the Rayleigh-Sommerfeld (R-S) integral[18-19], boundary diffraction wave theory[20], Gaussian beam decomposition algorithm[21], etc. Deviation between classical theory and rigorous vector theory in predicting focal properties becomes obvious with the miniaturization of device dimension[22-23], hence, vector analysis models are utilized among other rigorous calculation method[24-27]. We hereby employed a full 3D FDTD package[28] to model the silicon MLAs because of its high accuracy and compatibility with many complex structures.

The structure parameters of the simulated multistep microlens were obtained based on optical path difference (OPD) using a traditional scalar method[29]. In order to explore the focal shift in MIR wavelength band, 4.2 μm was chosen as the center illumination wavelength in the simulation setup, which is in the center of the mid-infrared atmospheric window, the incident bandwidth of 0.5 μm.

The basic simulation setup is shown in Fig. 1: the MIR plane wave is incident vertically upon the multistep surface of silicon MLAs, the curved wavefront caused by these steps leads to focusing effects within the Si substrate. As can be seen in Fig. 1, the focal spot of absolute power intensity (FDTD focus, known as actual focal spot) does not coincide with the geometric focal spot (Geometric focus), but shifted along the z-axis toward the microlen surface. A focal depth of about 25 μm (227 ~252 μm) can be found for this microlen structure with a low Fresnel number N.

Several papers tried to address the focal shift theoretically for microlens in low-Fresnel-number systems[20, 30-32], where the focal shift is defined as $\Delta f = f - f'$, f is the geometric focal length, and f' is the FDTD focal length. These theories, which derived from visible or near-infrared wavelength, provided limited validity when predicting the focal shift in this simulation setup with the incident wavelength being MIR. Formulas in these papers suggested a relative focal shift ($\Delta f/f$) of about 0.26 ~0.28 for structure in Fig. 1 with a Fresnel number of $N = 1.49$ (the Fresnel number is defined by $\alpha^2/\lambda f$, f number $\gamma = 4$, which is defined by $f/2\alpha$, where α and λ are the radius of microlens pitch and operational wavelength respectively). For comparison the value obtained by 3D FDTD is about 0.37 ~0.43, as shown in Fig. 1. As we can see there is a pronounced mismatch between the focal shift obtained by FDTD and that from previous models. We attribute this mismatch to the limited validity of classical theory: with the decrease of physical dimension of the MLAs to the wavelength scale and the extension of the incident wavelength band to MIR, rigorous analysis method must be utilized in order to model the focal length of these optical devices more accurately.

2 Fabrication and characterization

The Si MLAs were successfully fabricated, which required triple lithography alignments, with each followed by Induced Coupled Plasma (ICP) etching[9]. The etching depth was carefully controlled in order to construct an appropriate focusing wavefront. As we can see in Fig. 2, the steps obtained by etching show high fidelity in the design structure. The etching depth of each step h was 216 nm ($h = \lambda/(n-1)$, where $\lambda = 4.2$ μm, $n = 3.42$). The ring radius was calculated using Eq. (1),

$$r_m = \sqrt{\frac{2fm\lambda}{Nn} + \frac{m^2\lambda^2}{N^2n^2}}, N = 2^3, m = 1,2,\cdots,8 \quad . \quad (1)$$

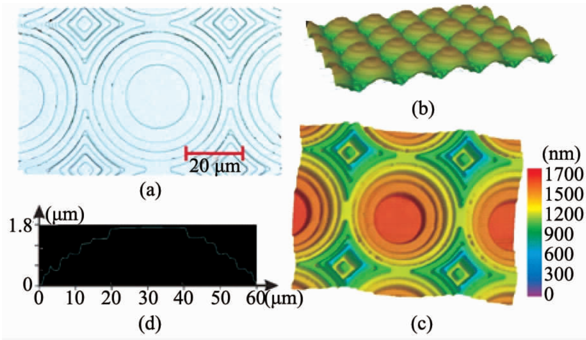

Fig. 2 3D laser microscope characterization of silicon microlens. (a) Optical photograph, top view. (b-c) Bird's eye-view and top view. (d) Measured cross section profile
图 2 硅微透镜 3D 激光显微镜表征(a)光学显微镜俯视(b-c)鸟瞰和俯视图(d)截面测试

We calibrated the etching parameters to get a smooth surface after etching. AFM measurement showed that the surface RMS increased with the etching depth, the largest RMS in the 8 *th* step was lower than 3 nm indicating that surface scattering can be neglected in our simulation. A ZnS thin film antireflective coating was then conducted to the back surface of the 400 μm thick silicon wafer using RF magnetron sputtering to minimize the reflective power loss.

3 Focal properties measurement

3.1 Experimental setup

Focal properties of the MLAs were experimentally studied on a horizontal "microscope" system. The silicon surface, with MLAs on it, was illuminated using collimated plane MIR wave emitting from a standard blackbody with band pass filter (4.25 ±0.25 μm). The focal spot behind the microlens was imaged with a high magnification onto an HgCdTe camera (InfraTec, ImageIR 8800 Series). As is shown in Fig. 3, the positions of the objective and camera were fixed. We adjusted the location of MLAs along optical axis. By doing this we set the front focal plane of objective at the surface of the silicon MLAs. This focal plane can be confirmed when a clear image of the surface structure, i. e., the concentric circles making up the array were observed by the camera. As is known, it is difficult to obtain high resolution images of the microlens structure in detail at the resolution of one or two μm using only one set of objective, especially with the illumination incident wave being MIR. The position of the microlens was hence adjusted using a 3D step stage, by displacing the MLAs towards positive *z* direction. As the silicon surface was illuminated by a plane wave, the diffraction pattern within the silicon substrate ($z<0$) didn't change with respect to the microlens surface. As a result, a series of diffraction patterns at different location within the silicon substrate were captured with the displacement of the MLAs.

As is shown in Fig. 3, while the position of a microlens was adjusted along the optical axis, different diffraction patterns within the microlens substrate were obtained. The position of the image plane was recalculated to account for refraction of imaging light at the output Si/air surface and thus the diffraction pattern of focusing light was mapped along z-axis. The images obtained using the HgCdTe camera were then generated by the digital voltage of an incident signal, which needs to be transformed to the equivalent blackbody temperature to generate the power distribution of each picture by integral of blackbody radiation formula at these temperatures.

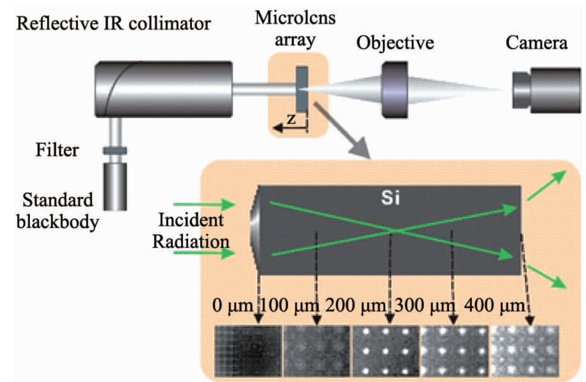

Fig. 3 Experiment setup of focal properties measurement
图 3 聚焦特性实验测试示意图

3.2 Measurement results

Focal power intensity ($I(z)$), as is shown in Eq. 2, was generated by the integral of power pattern (E) within the spot area with the diameter (d) from the inset of Fig. 4, and then plotted at 8 discrete z-vertical planes along the incident direction (red circle markers). The power intensity along optical axis was calculated using the FDTD in Part 2 (black solid line). Power patterns at different *z* planes were captured from the plane of the MLAs surface all the way to the backside surface of silicon wafer.

$$I(z) = \int_0^{d/2} E\mathrm{d}s \quad . \quad (2)$$

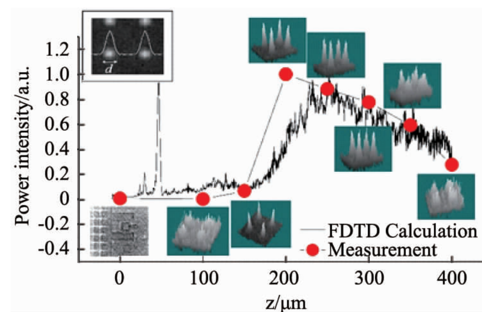

Fig. 4 Maximum power intensity of focusing light along optical axis of microlens
图 4 汇聚光强最大值随着微透镜光轴变化

In Fig. 4, measurement results show good agreement with FDTD simulation, thus conforming a focal shift at the range of 0.37 ~ 0.5 (FDTD simulation: 0.37 ~ 0.43, measurement: 0.5). We attribute the mismatch

(~20 μm) between simulation and measurement to the limited accuracy of the measurement system. It is difficult, if possible, to obtain an accurate z-axis position of the front objective focal plane with respect to the MLAs on the order of the illumination wavelength (~ 4.2 μm). We therefore conclude that the focal shift in the MIR MLAs is much larger than that predicted by traditional models. One must use rigorous electromagnetic models to decide the focal length of MLAs in order to incorporate other micro-nano optical systems.

Fabrication errors mainly came from mask misalignment and etching step height deviation. Normal manual mask aligner was used during the fabrication, the average mask alignment accuracy was around 1 ~ 2 μm. Due to the in plane radical and angular misalignment, it's normal that the individual microlens at different areas within the same wafer can exhibit slightly different lateral structures; concentric circles in Fig. 2(a) become non-concentric. During the measurement, different areas within the wafer were tested. In terms of focal length no noticeable difference was found. As a result we believe that the non-uniformity caused by mask alignment error have minor effects on the focal shift. It also agrees with the Effective Medium Theory[33] that index profile of each local point can be approximated by averaging the surrounding fractions. Minor deviation of the structures does not affect the overall refractive index profile. 3D FDTD was used to evaluate how step height etching error can effect focal shift. It showed that larger step height could lead to shorter focal length, as light will experience more phase delay and thus lead to a more converging wavefront, vice versa. Surface roughness caused by ICP has no effect on the focal shift, however it can decrease the transmission efficiency due to absorption and additional diffuse scattering.

4 Conclusions

The focal shift of the silicon microlens in the mid-infrared regime was numerical modeled and experimentally verified. We found that traditional methods provide limited validity in predicting the focal length of MLAs with small critical size and in long wavelength bands. As a result rigorous electromagnetic method (3D FDTD) was employed to model the focal shift effect of MLAs in mid-infrared regime. Numerical calculation revealed a more pronounced focal shift with a factor of about 0.37 ~ 0.43. We have also traced the focal shift of MLAs in mid-infrared regime experimentally and confirmed the simulation. The effects of fabrication error and surface roughness on focal shift were also discussed. The rigorous calculation method in this paper provides a reference value to account with a focal shift effect in micro-nano optical devices with the critical dimension on the order of the wavelength scale. Moreover, the demonstration of the focal properties measurement also provides ways to characterize the focusing effect experimentally in MIR.

Our results are of practical value in the integration of micro-nano optical systems, such as incorporation of MLAs in mid-infrared focal plane array (IRFPA), where distortion in predicting the focal length of the silicon microlens between traditional theory and rigorous model becomes significant due to the miniaturization of the device size. In these cases the focal length of MLAs must be confirmed using rigorous electromagnetic methods and measured experimentally. In this way the focal spot of incident power will be located exactly at the photosensitive area of photodetector, thus improving the detection efficiency of IRFPA.

Acknowledgments

This work was supported by the Special Project on the Integration of Industry, Education and Research of Aviation Industry Corporation of China.

References

[1] Kumaresan Y, Rammohan A, Dwivedi P, *et al*. Large area IR microlens arrays of chalcogenide glass photoresists by grayscale maskless lithography[J]. *ACS Appl. Mater. Interfaces*, 2013. **5**(15):7094.

[2] Zhang L, Ma X Z, Zhuang J L, *et al*. Microfabrication of a diffractive microlens array on n-GaAs by an efficient electrochemical method[J]. *Adv. Mater.*, 2007. **19**(22): 3912-3918.

[3] Deng Z F, Chen F, Yang Q, et al. Dragonfly-eye-inspired artificial compound eyes with sophisticated imaging[J]. *Adv. Funct. Mater.*, 2016. **26**(12): 1995-2001.

[4] Agranov G, V Berezin, R H Tsai. Crosstalk and microlens study in a color CMOS image sensor[J]. *IEEE Trans. Electron Dev.*, 2003. **50**(1):4-11.

[5] Guo N, Hu W D, Chen X S, *et al*. Optimization of microlenses for InSb infrared focal-plane arrays[J]. *J. Electron. Mater.*, 2011. **40**(8): 1647-1650.

[6] Binnie T D. Fast imaging microlenses[J]. *Appl. Opt.*, 1994. **33**(7):1170-1175.

[7] Liu H W, Chen F, Yang Q, *et al*. Fabrication of bioinspired omnidirectional and gapless microlens array for wide field-of-view detections [J]. *Appl. Phys. Lett.*, 2012. 100(13): DOI: 10.1063/1.3696019.

[8] Huang T F, Hua S H, Hu K C, *et al*. LED chip having micro-lens structure[P]. 2012, Google Patents.

[9] Stern M B. Binary optics: A VLSI-based microoptics technology[J]. *Microelectron. Eng.*, 1996. **32**(1-4): 369-388.

[10] Li Y J, Wolf E. Focal shifts in diffracted converging spherical waves [J]. *Opt. Commun*, 1981. 39(4): 211-215.

[11] Hu B, Wang Q J, Zhang Y. Systematic study of the focal shift effect in planar plasmonic slit lenses. Nanotechnology, 2012. **23**(44): 444002.

[12] Gao Y, Liu J L, Zhang X R, *et al*. Analysis of focal-shift effect in planar metallic nanoslit lenses[J]. *Opt. Express*, 2012. **20**(2):1320-9.

[13] Hernandez-Aranda R I, Gutierrez-Vega J C. Focal shift in vector Mathieu-Gauss beams[J]. *Opt. Express*, 2008. **16**(8): 5838-48.

[14] Verslegers L, Catrysse P B, Yu Z F, *et al*. Planar lenses based on nanoscale slit arrays in a metallic film[J]. *Nano Lett.*, 2009. **9**(1): 235-238.

[15] Aristov V, Grigoriev M, Kuznetsov S, *et al*. X-ray refractive planar lens with minimized absorption[J]. *Appl. Phys. Lett.*, 2000. **77**(24).

[16] Yamazaki R, Obana A, Kimata M. Microlens for uncooled infrared array sensor[J]. *Electronics and Communications in Japan*, 2013. **96**(2):1-8.

[17] Deng Z F, Yang Q, Chen F, *et al*. Fabrication of large-area concave microlens array on silicon by femtosecond laser micromachining[J]. *Opt. Lett.*, 2015. **40**(9):1929-1930.

[18] Liu Y L, Liu H. Analysis of a diffractive microlens using the finite-difference time-domain method[J]. *J. Micro-Nanolith Mem*, 2010. **9**(3).

[19] Gao H W, Hyun J K, Lee M H, *et al*. Broadband Plasmonic Micro-

lenses Based on Patches of Nanoholes[J]. *Nano Lett.*, 2010. **10**(10): 4111-4116.
[20] Li Y. Dependence of the focal shift on Fresnel number and F-Number[J]. *J. Opt. Soc. Am.*, 1982. **72**(6).
[21] Arnaud J. Representation of Gaussian beams by complex rays[J]. *Appl. Opt.*, 1985. **24**(4): 538-539.
[22] Schmitz M, Bryngdahl O. Rigorous concept for the design of diffractive microlenses with high numerical apertures[J]. *J. Opt. Soc. Am. A*, 1997. **14**(4): DOI: 10.1364/JOSAA.14.000901.
[23] Pomme D A, Moharam M G, Grann E B. Limits of scalar diffraction theory for diffractive phase elements[J]. *J. Opt. Soc. Am. A*, 1994. **11**(6): 1827-1830.
[24] Prather D W, Shi S Y. Formulation and application of the finite-difference time-domain method for the analysis of axially symmetric diffractive optical elements[J]. *J. Opt. Soc. Am. A*, 1999. **16**(5): DOI: 10.1364/JOSAA.16.001131.
[25] Lin L, Goh X M, McGuinness L P, , *et al*. Plasmonic lenses formed by two-dimensional nanometric cross-shaped aperture arrays for Fresnel-region focusing[J]. *Nano Lett.*, 2010. **10**(5): 1936-1940.
[26] Vaillant J, Crocherie A, Hirigoyen F, *et al*. Uniform illumination and rigorous electromagnetic simulations applied to CMOS image sensors[J]. *Opt. Express*, 2007. **15**(9): 5494-503.
[27] Prather D W, Shi S Y. Combined scalar-vector method for the analysis of diffractive optical elements[J]. *Opt. Eng.*, 2000. **39**(7).
[28] Taflove A, Hagness S C. *Computational electrodynamics*[M]. Artech house, Boston, 2000.
[29] Mait J N. Understanding diffractive optic design in the scalar domain[J]. *J. Opt. Soc. Am. A*, 1995. **12**(10).
[30] Li Y J. A high-accuracy formula for fast evaluation of the effect of focal shift[J]. *J. Mod. Opt.*, 1991. **38**(9).
[31] Ruffieux P. On the chromatic aberration of microlenses[J]. *Opt. Express*, 2006. **14**(11): 4687-4689.
[32] Szapiel S, Scharf T, Herzig H P, et al. Marechal intensity formula for small-Fresnel-number systems[J]. *Opt. Lett.*, 1983. **8**(6).
[33] Niklasson G A, Granqvist C G, Hunderi O. Effective medium models for the optical-properties of inhomogeneous materials[J]. *Appl. Opt.*, 1981. **20**(1).